Droplet Electro-Bouncing in μ-Gravity

Erin S. Schmidt, Mark M. Weislogel

Abstract

Notes on electric fields 'n stuff.

1 Introduction

1.1 Spontaneous Droplet Jump

When a nonwetting, gravity dominated sessile drop or puddle initially at rest in the Cassie-Baxter state on a surface undergoes a large step reduction in Bond number, $\mathbf{Bo} = \rho g V_d^{2/3}/\sigma$, where ρ is the liquid density, g is the acceleration of gravity, V_d is the droplet volume, and σ is the liquid surface tension, it will spontaneously jump away from the surface. This was first observed experimentally by Kirko *et al.* in 1970 [ref] and later by Wollman *et al.* in 2006 in a set of experiments conducted using a μ-gravity drop tower [ref]. The kinetic energy of the jump is supplied by the defect in free surface energy as the new minimum energy surface equilibrium has approximately constant curvature [ref]. If the viscous energy losses by shear, and internal flows during roll up are neglected, as well as energy lost due to the hysteresis of the dynamic contact line, then the energy relation is given by

$$KE = SE_2 - SE_1 = [(\sigma A)_{gl} + (\sigma A)_{sg}]_2 - [(\sigma A)_{ls} + (\sigma A)_{gl} + (\sigma A)_{sg}]_1.$$

From this is derived a simple model for the droplet initial jump velocity, given by

$$U_0 = \left(\frac{\sigma g}{\rho}\right)^{1/4} \left[1 - \cos\theta + 2\left(\frac{\pi H^3}{V_d}\right)^{1/2} - 6^{2/3}\left(\frac{\pi H^3}{V_d}\right)^{1/3}\right]^{1/2},$$

where [etc, etc, etc...].

The droplet 'rolls up' as it jumps away from the surface due to radial motion of capillary wave away from the contact line. The characteristic time scale of the rolling up scales as $t_j \sim R_p/U\ (\rho H R_p^2/\sigma)^{1/2}$ [ref], which resembles the contact time, $\tau \approx 2.6(\rho R_d^3/\sigma)^{1/2}$ reported by Richard *et al.* in 2002 for the related problem of droplets impacting hydrophobic surfaces in 1-g [ref]. For droplets with radial symmetry and sufficiently high initial **Bo** these waves coalesce as a shock leading to geyersing and creation of satellite drops by the Rayleigh-Plateau breakup of the geyser. In the case of smaller jumping droplets, the capillary waves do not lead to geyersing, and are viscously damped to varying degrees during the brief freefall period of the drop tower.

The spontaneous droplet jump phenomenon provides a useful window though which to study the dynamics of large-lengthscale capillary dominated droplets. The governing physics of such massive droplets (far beyond the 1-g sub-millimetric capillary lengthscale) utterly defy terrestrial expectations about the ways in which liquid droplets 'should' behave, and also are of critical importance in a space exploration setting where the design of practical μ-gravity multiphase fluidic systems will no doubt be needed as humankind gradually extends her domain into our solar system.

2 Bouncing

For the sake of brevity we will henceforth use the slightly confusing term 'drop' as shorthand to refer to a single μ-gravity drop tower experiment.

3 Experimental Methods

Superhydrophobic substrates were placed on a drop tower rig platform. The rig is released by a solenoid chucked pin at the same moment the exterior drag shield is allowed to fall. This decouples drag acceleration felt by the drag shield from the experiment which experiences approximately $1 \cdot 10^{-6}$g of high quality freefall for the 2.1s required for the rig/drag shield assembly to reach the bottom of drop tower 6 floors below.

The superhydrophobic surface was treated with PTFE spray for the first experiment of the day, and approximately every 3^{rd} drop following. The general properties and details of the fabrication of these superhydrophobic surfaces are discussed in Section 3.1. Shortly before each drop the surfaces were briefly rinsed with distilled water, and then dried under a fume hood for about 10 minutes. The drop rigs were balanced to prevent unintentional torques from contaminating the kinematics data (as angular velocity of the camera-fixed inertial reference with respect to the droplets during freefall would appear as a linear acceleration of the droplet). Surface charge density was measured on the superhydrophobic surface using a *Simco-Ion* FMX-004 electrostatic fieldmeter. This measurement was done with the superhydrophobic surfaces connected by a conductive ground plane by conductive

tape, far away from the presence of other conductors. Some additional notes on idiosyncrasies of determining surface voltages (and thence surface charge densities) on insulative dielectric surfaces are provided in Appendix **??**.

Droplets of distilled water, in a range of volumes ($0 \leq R_d \leq 1$mL), were very carefully deposited on the superhydrophobic surface in the final 1-5 minutes prior to the drop using an ungrounded glass syringe with $\pm 1\mu$L accuracy. Red tracer dye was added to improve trajectory digitization. During the drop, droplet trajectories were observed using a *Panasonic* HC-WX970 Camera, shooting in high-speed mode at 120 fps and and 1/3000s shutter speed. In a few cases where higher frame rates were needed a *Nikon* 1 J1 camera with a 30mm telephoto lens was used, shooting at 400 fps. The experimental test cell was illuminated with a 12V 6000K *SEALIGHT* Chip-On-Board LED strip with a thin semi-opaque plastic film covering to make the light diffuse. The effect of static charges on spontaneously jumped droplet trajectories was studied in terms of the parameters droplet volume V_d, surface charge density σ, and a dependent variable, initial droplet jump velocity U_0. Since q cannot be directly measured insitu during a drop (as high-input resistance electrometers, being notoriously fickle instruments, are not well suited to sudden 15-g decelerations), it was inferred from the statistical distribution determined in corollary experiments. The droplet charge determination is discussed in slightly more detail in Appendix A.

3.1 Superhydrophobic surfaces

Wetting hysteresis. Methods of fabrication, comparison of wetting properties. Comparison of jump velocities between surfaces. Methods for determination of properties, roll-off angle, contact angle using *SE-FIT*. Cassie-wenzel transition. Damping. Droplets are dyed red to improve the quality of image thresholding when digitizing the droplet trajectories during data reduction.

3.2 Data Reduction

Digitization of droplet trajectories requires several steps of post-processing. Video is first decomposed into a sequence of still images. Trajectories are captured using the particle tracking module in *Fiji*[ref], a derivative of the popular *ImageJ*[ref] package for scientific image analysis. The series is stabilized to remove the effect of drop transients from the kinetmatic data[ref]. The series of still images is cropped, and the background (that is, the low-entropy pixels) of the series is removed using a builtin "rolling ball" algorithm. Each still is then split into its constituent RGB maps. In this case the green channel images contained the most information, so these were then globally thresholded using the Triangle algorithm to recover a map of the pixels corresponding to the droplet's approximate position in the original still. Finally ellipses are fitted to the pixel map stepping through the time series to determine the positions of the centroid, and the semi-major and minor axes of the droplets during the drop. The results of the particle capture in *Fiji* are shown in Figure **??**. Out of plane motion for 'weakly 3D' trajectories is inferred from the change in tracked area of the droplet. Droplet positional

data was smoothed ex post facto using a Savitsky-Golay filter. Additional details regarding the data smoothing methodology are presented in Appendix ??.

4 EHD Forces

As previously speculated the the force acting on the droplets as a surrogate for gravity are likely electrohydrodynamical in origin. In the hopes of unraveling the underlying mechanism for the electro-bouncing we turn to the electrodynamical approximation of fluids under the influence of electric fields. To that effect, what follows is a condensed overview of mathematical description of basic electrohydrodynamic flows. We first assume a DC electric field, such that $Re\langle\epsilon\rangle \approx$ constant, where ϵ is the dielectric permittivity of the respective media. We also assume that currents are small such that the effects of magnetic fields can be neglected. For the validity of this assumption to hold the characteristic time scale for electrical phenomena $\tau_e = \epsilon\epsilon_0/\sigma_e \ll 1$, where we note that τ is the ratio of absolute dielectric permittivity $\kappa = \epsilon\epsilon_0$, to conductivity σ_e, of the medium [ref]. Given the respective conductivity, and permittivity of air ($\sigma_e = 2.5 \cdot 10^{-16}\ \Omega^{-1}cm^{-1}$), we estimate $\tau_e \approx 400$s. This assumption also allows us to assume that the net charge present in the medium surrounding the droplets remains approximately constant during the typical time interval of a μ-gravity experiment, and no transfers of charge occur after the droplet leaves the surface. [lol, check these numbers...]

4.1 Maxwell Stress

If we suppose that electrical forces acting on free charges and dipoles in a fluid are transferred directly to the fluid itself, then this overall electrical body force will be the the divergence of the Maxwell stress tensor τ_m, by

$$\mathbf{F}_e = \nabla \cdot \tau_m = \nabla \cdot \left(\epsilon\epsilon_0 \mathbf{E}\mathbf{E} - \frac{1}{2}\epsilon\epsilon_0 \mathbf{E} \cdot \mathbf{E}\delta \right),$$

where $\mathbf{F}_e$ is the electric body force per unit volume, ρ_f is the free charge density, and δ is the delta function. The product of the electric field vectors is the dyadic product.

The classical Korteweg-Helmholtz force density formulation of the Maxwell stress tensor is usually expressed as

$$\mathbf{F}_e = \rho_f \mathbf{E} + \frac{1}{2} |\mathbf{E}|^2 \nabla\epsilon - \nabla \left(\frac{1}{2}\rho \left(\frac{\partial \epsilon}{\partial \rho} \right)_T |\mathbf{E}|^2 \right), \tag{1}$$

and ρ is the density of the dielectric fluid[ref].

The first term in this expression, equivalently written as $q\mathbf{E}$, is the well known Coulombic force or electrophoretic force, which arises from the presence of free charge in an external electric field. The second term is the force arising from polarization stresses due to a nonuniform field acting across a gradient in permittivity. This force is widely termed the dielectrophoretic force (DEP). The third term describes forces due to electrostriction, however in our case $\left(\frac{\partial \epsilon}{\partial \rho}\right)_T = 0$ due to the incompressibility of the fluid[ref]. While it is a relatively rigorous approach, and a useful conceptual model, evaluating the force density in this fashion can be somewhat onerous.

4.2 Dielectrophoresis

An alternative approximation for the polarization stress is to idealize the droplet as a simple dipole using the effective dipole moment method first suggested by Pohl and Jones[ref][ref]. This approach can be related back to the force density by means of a Taylor series expansion of $\mathbf{E}$ in the limit of a small gradient [ref]. The DEP force is distinct from the Coulombic force in that net charge is not required, and that the force vector goes in the direction of steepest descent of the field, $\nabla |\mathbf{E}|^2$, rather than in the direction of $\mathbf{E}$. The DEP force is related to the dipole moment (induced or polarized) of polarizable media which has a tendency to align the dipole with the electric field. If there is a gradient in the field then for a finite separation of charge one end of the dipole will feel a stronger electric field than the other, resulting in a net force. Whether the force is positive or negative in the direction of the electric field gradient depends on the difference of dielectric permittivites between the fluids, rather than on the polarity of $\mathbf{E}$. It bears repeating that droplets will polarize in a uniform field, but since there is no gradient in the field the forces felt by the dipoles are symmetric and there is no net force. The dipole moment of a spherical dielectric particle immersed in a dielectric medium is given by

$$\mu = V_d \mathbf{P} = \frac{4}{3}\pi R_d^3 \mathbf{P}, \tag{2}$$

where $\mathbf{P} = (\kappa_1 - 1)\,\epsilon_0 \mathbf{E}_{iz}$ is the polarization moment, and R_d is the particle radius, (κ_1 being the relative dielectric constant of the medium, and $\mathbf{E}_{iz}$ is the z-coordinate component of the electric field internal to the sphere, assuming the external electric field to be oriented parallel to the z-axis). The excess

polarization $\mathbf{P}_e$, in the sphere is given by

$$\mathbf{P}_e = (\kappa_2 - \kappa_1)\,\epsilon_0 \mathbf{E}_{iz} = \frac{3\kappa_1}{\kappa_2 + 2\kappa_1}\mathbf{E}_{iz}, \tag{3}$$

where κ_2 is the dielectric constant of the particle. Taking together equations 2, and 3 we find that the effective dipole moment of the particle is given by

$$\mu = 4\pi R_d^3 \left(\frac{\kappa_2 - \kappa_1}{\kappa_2 + 2\kappa_1}\right) \kappa_1 \epsilon_0 \mathbf{E}, \tag{4}$$

and the force felt by the dipole is

$$\begin{aligned} \mathbf{F}_{dep} &= (\mathbf{P}_e \cdot \nabla)\,\mathbf{E} & (5)\\ &= 2\pi R_d^3 \kappa_1 \epsilon_0 \left(\frac{\kappa_2 - \kappa_1}{\kappa_2 + 2\kappa_1}\right) \nabla E^2, & (6) \end{aligned}$$

where it is a useful shorthand to refer to the permittivity ratio by $K = \frac{\kappa_2 - \kappa_1}{\kappa_2 + 2\kappa_1}$, which is also known as the Clausius-Mossotti factor. In cases where $K < 0$, or $K > 0$ the particle will be repelled or attracted to regions of strong field respectively. In our experiment, taking the relative dielectric constants to be $\kappa_1 \approx 1$ and $\kappa_2 \approx 80$, we have $K \approx 0.96$. One limitation of the effective dipole moment approximation of the DEP force is that it requires an assumption of small physical scale of the particle relative to the lengthscale of nonuniformity of the field, which in this case we take to be the length of the charged superhydrophobic surface ($L, H = 25\text{mm} \gg a \approx 2.5\text{mm}$). Though the effective dipole moment is a successful model due in large part to its simplicity, it can be readily extended to include higher-order multipole effects, and non-spherical particles (oblate and prolate spheroids).

An excellent summary of DEP theory in terms of the effective dipole moment is given in [ref]. [Some notes on scaling ...]

4.3 Forces due to Image Charges in the Dielectric

5 The Electric Field

We are faced with the need to compute the total electric field arising from the presence of free charge on the surface of a polarizable dielectric. In the electrostatic case we have

$$\nabla \times \mathbf{E}(\mathbf{r}) = 0 \tag{7}$$

$$\nabla \cdot \mathbf{D}(\mathbf{r}) = \rho(\mathbf{r}). \tag{8}$$

If the dielectric is linear and isotropic then the displacement field is

$$\mathbf{D}(\mathbf{r}) = \epsilon(\mathbf{r})\mathbf{E}(\mathbf{r}). \tag{9}$$

Given that the electric field is defined as the gradient of the scalar potential, $\mathbf{E} = -\nabla\varphi$, we can write equation 9 as

$$\nabla \cdot [\epsilon(\mathbf{r})\nabla\varphi(\mathbf{r})] = -\rho(\mathbf{r}). \tag{10}$$

This is a form of *Poisson's equation*. Our general method for finding the electric field, will solve $\varphi(\mathbf{r})$ on a half-space domain with permittivities ϵ_1, ϵ_2 for a point source using the free-space *Green's function*. We can then find

the total electric field by superposition of the individual Green's functions by direct integration.

The non-homogoneous part of the Poisson's equation for the electrostatic potential is a Green's function, denoted by $\mathbf{G}(\mathbf{r}|\mathbf{r}')$, where $\mathbf{G}$ satisfies Poisson's equation at $\mathbf{r}$ when the point source is located at $\mathbf{r}'$ such that

$$\nabla^2\mathbf{G}(\mathbf{r}|\mathbf{r}') = -\delta(\mathbf{r}-\mathbf{r}'). \tag{11}$$

Using the identity for the position vector ∇

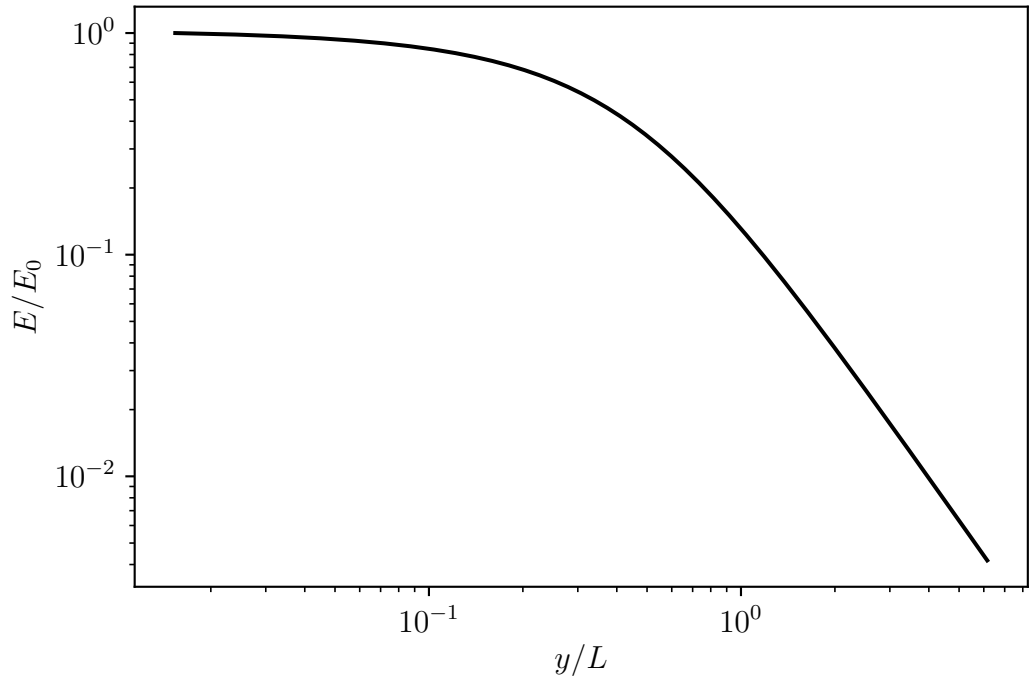

Figure 1: A simple EMA plot.

6 A Simple Dynamical Model

6.1 Trajectory Equation

6.2 Numerical Methods

7 Comparisons

8 Stability

9 Conclusions

A

Droplet Charge

Parallel Plate Method

Since, by the earlier scaling, we presuppose the source of the droplet bouncing behavior to be primarily Coulombic in origin (as opposed to dielectrophoretic), the droplet must have some net charge in addition to the charge induced by the electric field. To measure this charge concurrent methodologies were used. The first method of determining the droplet net charge is observation of the deflection of the droplets in the region of a known uniform field in a fashion inspired by Millikan's famous experiment to determine the fundamental charge of the electron [ref].

Droplets were jumped in freefall from a sandpaper superhydrophobic sur-

face placed between the plates of a parallel plate capacitor of known uniform electric field. The surface was first deionized using a balanced *Ptec* IN5120 DC air-ionizer to remove the effect of surface charge of the superhydrophobic surface from perturbing the otherwise uniform field set up between the parallel plates. A schematic of the parallel plate drop apparatus is shown in Figure **??**. Since the droplet initial velocity U_0 is parallel to the electric field, the droplets are inertial in the direction of the electric force, and neglecting the effect of image charges mirrored across the conductors, we can determine the magnitude of the droplet charge by a balance of Coulombic force and inertia given by the equation of motion

$$\frac{d^2y}{dt^2} = q\mathbf{E}.$$

Since the drag is negligible in the inertial limit we can find the charge q by fitting a second-order least squares polynomial to the measured droplet positions, equating the t^2 term to the constant acceleration, and dividing by the known, constant magnitude of the electric field. From a survey of literature we suppose the droplet charge, if they are indeed charged by contact with PTFE, to be some function of the droplet volume and the residence time on the superhydrophobic surface. However, sweeping though droplet volumes over a series of drop tower experiments we find little correlation between droplet volume and net droplet charge. This is shown in figure **??**.

A 200-880 VAC source with a full wave bridge rectifier circuit was prototyped on perf-board for initial experiments to measure droplet charge. The circuit was analyzed on an laboratory oscilloscope to verify that the AC com-

ponent of the signal was appropriately small (13 mV at 35 kHz). Current was determined to be a relatively low 80 μA. The high-voltage source terminals were led to two parallel polished 150x150 mm aluminum plate electrodes. The electrodes were mounted on an insulated 80/20 extruded aluminum rail for ease of adjustment. All droplet charge experiments were conducted with an electrode spacing of 28.30 mm. With this spacing the calibrated electric field between the plates was $\mathbf{E} \approx 35\text{kV/m}$. The electrodes were electrically isolated from the drop rig by two alternating layers of 4 mm thick laser cut acrylic sheet and Kapton tape. Potential across the plates was measured periodically with a load-impedance corrected multimeter to account for battery depletion. The typical capacitor rise time of the plates was measured to be 1.4 s, thus to make the most economical use of the brief window a microgravity a weighted switch was set by hand prior to the drop to close the high-voltage circuit, but which passively safed the system at the resumption of 1-g conditions in the tower. The drop apparatus is shown in Fig.

A brief screening experiment was conducted which alternated the polarity of the field by switching the positive and negative terminal leads between plates. Qualitative observations of droplet electrode preference seem to indicate that the assumption of small polarization stress was well founded. Following this a orthogonal array 3^2 factorial design experiment with two replicates was conducted to test the effect of varying droplet volume and surface stay time on net charge at the time of jumping. It was hypothesized in accordance with previous studies [**?**], that net charge would increase for levels of both factors. The results of the factorial experiment are presented in Fig. **??**. ANOVA analysis in R of the linear multiple regression model for

the data set indicates that neither droplet volume ($p = 0.105$), nor surface stay time ($p = 0.358$) is significant at the 95% confidence level. The overall model F-statistics (2.177 in 2 and 13 degrees of freedom), and coefficients of determination ($r^2 = 0.2509$) indicate that the linear model neither fits the data particularly well, nor does it offer an improvement over the mean model. The mean charge was determined to be positive $2.3 \cdot 10^{-11}$ C, with a standard deviation of $1.8 \cdot 10^{-11}$ C.

The failure of the model to describe the data raises interesting questions about the validity of our initial assumptions. Typical Reynolds numbers ($R_e = 280$ average) indicate the general validity of the assumed quadratic drag model. The drag scale quantity given by Eqn. **??** was much less than 1 for all test runs, with mean value of $1.0 \cdot 10^{-2}$ and a standard deviation of $2.0 \cdot 10^{-3}$, which adds credence to a force balance of pure inertia and electrostatic force.

One obvious issue, in retrospect, is that while we know the characteristic charging time for the droplets to be some function of droplet volume, [it has been shown to have a time constant dramatically smaller than that of a typical experimental timescale] so we might have looked only for the charge as a function of volume, both on physical grounds and due to the conflation of the variables.

Also of concern is that droplets in three of eighteen runs exhibited accelerations opposite to the expected direction. There is no pattern to the distribution of anomalous droplet accelerations, as they all occurred at unique level combinations. There are only four obvious ways of explaining this anomaly. The first is that the electric field is in fact non-uniform and polarization stress

is non-negligible in this geometry. This option seems unlikely owing to the fundamental design of the experimental apparatus; [see figure from Agros2D FEM solution]. A second possibility is that the few contrarian droplets actually accumulated net negative charge, instead of the net positive charge to be expected on the basis of evidence from some of the aforementioned studies. This is not impossible, and would also go some length to explain the variance in the measured charge generally. A third possibility is that another force neglected in this analysis, with some component in the direction opposite of the electric field, has an $\sim \mathcal{O}(1)$ magnitude. In principle this could for instance include the image charges which will subject the droplets to a force $\mathbf{F} = q^2/4\pi\epsilon_0 d$ when "close" to one of the conductive plates (that is, when the plate can be treated as an infinite grounded conductor). However, this formulation of the image charge effect clearly does not describe the force close to the centerline where the Green's function needs to add additional sets of images to satisfy the boundary conditions of $\nabla^2\varphi = 0$ in this geometry. To the knowledge of the author there is not a convergent series solution in the parallel plates geometry as yet.

The droplet positive net charge developed by contact with a PTFE surface corresponds to findings elsewhere in literature [?] [?] [?]. The smallest droplet size treated in the present work is several times larger than the largest in any of comparable study. The most relevant comparison found droplet static charge of 2.5e-10 C for 10 μL droplets charged by pipetting from a PTFE tipped needle [?]. The present results mean charge level of 2.3e-11 C is, within error, roughly six times smaller than the cited study.

Direct Measurement

A second approach to determining the net droplet charge is by direct measurement in a shielded Faraday cup using an extremely high input resistance electrometer, specifically a *Keithly* 616 digital electrometer. [note on operational philosophy, data collection]. Correlation of net charge to droplet volume is shown again for in figure ??.

[Discussion on discrepancy between the two approaches.]